

Experimental and Numerical Investigation of Weak, Self-Sustained Conditions in Engineered Smouldering Combustion

Marco A. B. Zanoni ^{a*}, José L. Torero ^b, Jason I. Gerhard ^a

^a Department of Civil and Environmental Engineering, University of Western Ontario, London, Ontario N6A 5B9, Canada

^b Department of Civil, Environmental and Geomatic Engineering, University College London, UK

* Corresponding author at: Department of Civil and Environmental Engineering, The University of Western Ontario, Spencer Engineering Building, Rm. 1041D, London, Ontario N6A 5B9, Canada. Cell: +1 (226) 236 9985. E-mail address: mbazelat@uwo.ca (M.A.B. Zanoni).

Abstract: Engineered smouldering applications require self-sustaining conditions where the fuel is consumed without any addition of energy beyond ignition. In practical applications, it is preferred to create scenarios that are robust (i.e., far from extinction). In this work, smouldering column experiments were conducted, spanning conditions from robust self-sustaining through weak self-sustaining and to extinction by systematically lowering the applied air flux and the fuel concentration. A previously developed one-dimensional numerical model, which was validated under robust smouldering conditions, was used to simulate the experiments. Experiments showed front deformation in the weak and extinction cases due to multi-dimensional effects. This deformation resulted in a redistribution of the air flow, altering the global energy balance at the centre-line. The model was found to be unable to accurately reproduce these weak and extinction cases with the original validation parameters. A sensitivity analysis revealed that treating the heat of combustion as a fitting parameter, and letting it vary beyond its realistic maximum, enabled the model to create a condition of sufficient energy at the centre-line and was the best way to quantitatively simulate the weak and extinction cases for this specific scenario. This reveals that the model assumptions,

particularly the assumption of one-dimensionality, are sufficient for robust smouldering but are insufficient for weakly self-sustaining scenarios.

Keywords: Smouldering Combustion, Bitumen, Porous Medium, Heat of Combustion, Heat Losses

Nomenclature

Latin Letters

A	Pre-exponential factor, s^{-1}
A_s	Surface area, m^2
C_p	Specific heat capacity, $J\ kg^{-1}\ K^{-1}$
d_p	Particle diameter, mm
D_g	Diffusion coefficient, $m^2\ s^{-1}$
E	Activation Energy, $kJ\ mol^{-1}$
\dot{E}	Energy rate, $J\ s^{-1}$
k	Thermal conductivity, $W\ m^{-1}\ K^{-1}$
k_p	Intrinsic permeability, m^2
L	Contaminated region length, m
\dot{m}_{O_2}	Oxygen mass flux, $g\ s^{-1}$
h_{sg}	Interfacial heat transfer coefficient, $W\ m^{-2}\ K^{-1}$
\dot{q}''	Heat flux, $W\ m^{-2}$
r	Radius, m
\dot{R}	Reaction rate, s^{-1}
R_g	Ideal gas constant, $J\ K^{-1}\ mol^{-1}$
S_b	Bitumen saturation
t_g	Air-on time, s
t_h	Heater-off time, s
T_p	Peak temperature, $^{\circ}C$
u_g	Darcy air flux, $m\ s^{-1}$
U	Global heat loss coefficient, $W\ m^{-2}\ K^{-1}$
V	Volume, m^3
v_c	Char yield coefficient
v_f	Front velocity, $mm\ min^{-1}$
ν_{O_2}	Oxygen stoichiometric coefficient, $kg\ O_2\ kg\ fuel^{-1}$
Y	Mass fraction

Greek Symbols

ΔH	Heat of oxidation, $MJ\ kg^{-1}$
ρ	Density, $kg\ m^{-3}$
σ	Stefan–Boltzmann constant, $W\ m^{-2}\ K^{-4}$
ϕ	Porosity

Subscripts/Superscript

add	Added
b	Bitumen
c	Char
cl	Cylinder

<i>eff</i>	Effective
<i>g</i>	Gas
<i>0</i>	Initial
<i>oxid</i>	Oxidation
<i>pyr</i>	Pyrolysis
<i>rad</i>	Radiation
<i>rem</i>	Removed
<i>s</i>	Solid/bitumen
<i>sp</i>	Sphere

1. Introduction

Smouldering is a flameless form of combustion where the oxidation reaction takes place on the surface of the condensed phase [1]. Natural smouldering typically occurs in porous solid fuels (e.g., peat [2]) and it is difficult to control and extinguish due to the reactive nature of the porous matrix and continuous air supply by means of natural convection. In engineered applications (e.g., soil remediation [3-7], waste management [8-11], energy conversion [12], sanitation [13, 14], and oil recovery [15]), smouldering requires forced air supply and the fuel (solid, sludge, or liquid) is embedded within a porous inert matrix. In the latter, practical parameters such as air flux, fuel and oxygen concentrations can be intentionally adjusted for process optimization [6].

Engineered smouldering requires self-sustained propagation to be maintained so that the fuel is consumed without any addition of energy beyond ignition. Furthermore, it is preferred to create scenarios that are highly robust, i.e., far from extinction [6, 16] and generating the maximum amount of excess energy for subsequent capture and use [12]. Zanoni et al. [6] showed that robust conditions are created when the global (i.e., bed or system) net energy rate (\dot{E}_{net}) is strongly positive, i.e., energy is released (\dot{E}_{add}) more quickly than energy is removed (\dot{E}_{rem}) [6, 17]:

$$\dot{E}_{net} = \frac{1}{L} \int_0^L (\dot{E}_{add}(l) - \dot{E}_{rem}(l)) dl \geq 0 \quad (1)$$

where L is the system length. Zaroni et al. [6, 17] showed that in Eq. (1), \dot{E}_{add} is the sum of the input energy rate from a heating source (\dot{E}_{heater}) and the oxidation energy release rate (\dot{E}_{oxid}), and \dot{E}_{rem} is the sum of the pyrolysis energy rate (\dot{E}_{pyr}), the energy rate from radial heat losses (\dot{E}_{loss}), and energy rate leaving the system at the outlet (\dot{E}_{out}). In numerical models, heat losses are typically expressed by a global heat loss coefficient (U), whereas oxidation is described by the product of heat of combustion (ΔH_c) and reaction rates (\dot{R}), with the latter being a function of temperature, fuel concentration, oxygen concentration, and oxygen mass flux. At self-sustaining conditions and far from the inlet and outlet boundaries, $\dot{E}_{heater} = \dot{E}_{out} = 0$; moreover, \dot{E}_{pyr} has been shown to be negligible [17]. Therefore, \dot{E}_{net} is primarily governed by \dot{E}_{oxid} and \dot{E}_{loss} , and the balance between them will dictate whether a smouldering system is self-sustaining ($\dot{E}_{net} \geq 0$), or trending towards extinction ($\dot{E}_{net} < 0$).

The most important conclusion of these studies is the identification of \dot{E}_{net} as the most relevant parameter describing the robustness of a smouldering reaction. The local energy balance at the reaction zone establishes whether the smouldering reactions exists or not. If the conditions are such that the Damköhler number exceeds a critical value, then the reactions will prevail [18-20]; if this is not the case, extinction will occur. Given that the smouldering reactions have high activation energies, extinction will be abrupt and irreversible (assuming no engineering interventions). In contrast, tracking \dot{E}_{net} provides the means to characterize the evolution of the robustness of the smouldering reactions as the Damköhler number decays. The time scale associated to the evolution of the energy in the reactor is not related to the reaction chemistry but to heat transfer (global energy balance) and therefore is long enough to enable changes to the operating parameters that can change the trajectory of the Damköhler number. While the Damköhler number remains local to the reaction zone and corresponds to the classical definitions [19, 20], the overall energy balance affects the ultimate temperature of the reaction, thus the characteristic time of the combustion chemistry. So, locally weak chemistry can continue if the Damköhler number remains above a critical value, but the decaying global energy balance slowly drives the reaction towards extinction

unless a change in operating conditions is enacted. Thus, the global energy balance allowed for the theoretical identification of a new regime of smouldering where the robustness of the reaction is sufficient to remain above extinction thresholds but is diminishing in time, at a rate much slower than the characteristic reaction chemistry times. Here, this regime will be named the “weak smouldering” regime and corresponds to conditions where \dot{E}_{net} is approaching zero but the Damköhler number remains above the critical value. A point that is important to be noted is the distinction between self-sustaining, non-self-sustaining and weak smouldering. Self-sustaining smouldering is when peak temperatures are constant or increasing while non-self-sustaining smouldering is when peak temperatures are diminishing. However, weak self-sustaining smouldering also shows peak temperatures decreasing with time, so weak self-sustaining and non-self-sustaining smouldering are hard to distinguish in the short term.

Experimental evidence of this weak regime is difficult to find. Smouldering front temperatures and propagation velocities are a function of a complex interplay of heat release and heat transfer, thus they do not provide direct evidence of the global energy balance. Therefore, the vast majority of experimental studies have characterized the weak smouldering regime only as an outcome of specific experimental conditions. An early study varied the supply of air to the reaction zone by using parabolic flights to reduce natural convection through cyclic variations of gravity [21]. It was noted that in the initial cycles the reaction recovered rapidly but as the reaction was exposed to more cycles, its capacity to recover diminished until extinction occurred. This is probably the first evidence that a weak smouldering regime exists but also that buoyancy could redistribute the air flow altering the global energy balance. Two other examples have been reported for the smouldering of polyurethane [22] and peat [2]. In the former, a possibly weak smouldering scenario, i.e., under oxygen-limited conditions, was reverted to robust conditions by increasing the initial oxygen concentration above ambient conditions. This resulted in more fuel consumption, thus the reaction was observed to have increased in strength. In the latter, two distinct

scenarios were observed. Near the surface, smouldering had a constant supply of oxygen, but was exposed to higher heat losses to the surroundings. When smouldering progresses in depth, the front was well-insulated but the oxygen supply decreased [2]. Both scenarios were identified as being weak and lead to extinction. Yerman et al. [9, 16] discussed smouldering robustness via an interplay between water evaporation and the chemical reaction front in the context of high moisture content fuels (e.g., feces). Robust conditions were reached when peak temperature and front velocity were stable and the evaporation front and reaction front were fully separated. Weak and extinction conditions were achieved when moisture content was high (56%), which resulted in a decrease in peak temperature and front velocity and in overlap of the evaporation and reaction fronts. These studies focused on the outcome but did not provide insight into the evolution of the processes towards extinction.

Numerical characterization of this regime is possible because all operating parameters can be varied independently. The sensitivity analysis presented by Zanoni et al. [6] showed that smouldering robustness was most sensitive to increasing fuel concentration, since this parameter can vary significantly and is directly proportional to the total energy released from oxidation when smouldering is within fuel limited conditions [6]. It is important to note that this scenario is different from the smouldering of porous solid fuels, where fuel density is constant and smouldering is limited by the oxygen supply [1].

The global net energy rate also increases with the mass flux of oxygen, i.e., either increasing oxygen concentration [2, 23] or air flux [6, 22, 24], until reaching excess oxygen conditions [6, 25]. Furthermore, increasing the heat of combustion, by addition of more energetic fuels, can also increase smouldering robustness [6, 26]. On the losses side of Eq. (1), increasing heat losses (e.g., poorly insulated systems) decreases the smouldering robustness [6, 26, 27]. While these studies served to identify the regime and to establish trends that describe the way in which the different operating parameters affect the weak smouldering reaction, none of these studies has revealed the physical phenomena that defines the evolution

of the weak smouldering regime. Therefore, there is still a need to define the processes that need to be modelled to properly characterize the weak smouldering regime.

Numerical models are typically validated under robust smouldering conditions and show limitations when used to predict smouldering extinction [5, 6, 17, 22, 26-28]. Given the complex coupling between the combustion chemistry and heat and mass transfer, it is difficult to establish the root of these limitations. Complex multi-dimensional models that include detailed chemistry and a refined treatment of the porous structure have been developed to understand the limiting conditions of smouldering [29-31]. Nevertheless, none of these models has been able to identify how combustion, heat and mass transfer evolve as smouldering enters the weak regime. The complex interactions of the multiple processes makes it challenging to establish the controlling mechanisms, thus it is beneficial to explore individual aspects numerically with simpler models coupled with experimental data.

A one-dimensional numerical model with simple (2-step) chemistry has been shown useful, providing important information about system energy balance, applied smouldering behaviour, trends, and sensitivity to key parameters [5, 6, 17]. While the model has only been validated against robust smouldering experiments [5], extending its application to the weak smouldering regime can help identify phenomena that need to be modelled in a more precise manner.

In this work, smouldering column experiments attempting to reproduce 1-D propagation were conducted spanning conditions from robust self-sustaining through weak self-sustaining to extinction. These changes were brought about by systematically lowering the applied air flux and the fuel concentration. These results were simulated with the previously developed one-dimensional numerical model described above [5]. When the model was found to be unable to accurately reproduce the weak and extinction cases with the original validation parameters, a sensitivity analysis was conducted. The purpose of the sensitivity analysis was to establish what processes the model was not accounting for. The simple description of the kinetic model and the flow within the porous medium allowed for a more transparent identification of

these processes. The sensitivity analysis revealed novel insight into how the model assumptions breakdown as the net energy balance decreases and served to identify the processes that need to be resolved in more detail.

2. Methodology

2.1. Experiments

Seven smouldering experiments (Table 1) were conducted in a stainless-steel column (Fig. 1). Experimental setup and methodology are described in detail in [5], and therefore only summarized here. The column contained 0.10 m of clean sand ($d_p=0.88$ mm) below the heater and a 0.35 m layer of a mixture of sand and bitumen (density (ρ_{bt})=1030 kg m⁻³, PG 58-28, McAsphalt Industry Limited) above it. Ten thermocouples spaced 0.035 m apart were assumed to measure the solid (sand/bitumen) temperature [32] along the column centerline every 2 seconds. The apparatus was insulated to minimize heat losses.

Experimental conditions ranging from mildly robust to weakly self-sustaining and then to extinction were attained by changing the air flux (u_g) and the bitumen content (described as saturation, the fraction of sand pore space occupied by fuel, S_b), Table 1. Each experiment was initiated by powering the resistive heater until the temperature at the first thermocouple ($x=0.12$ m) reached 400°C. Then air flux was supplied at t_g (Table 1), which initiated smouldering. The heater was then switched off at t_h (Table 1) while the air was maintained. The experimental time (t) was normalized for the purpose of comparing different experiments, and is referred to as Dimensionless Time ($DT=(t-t_g)v_f/L$, where v_f is the front velocity and L is the contaminated region length) [5, 33].

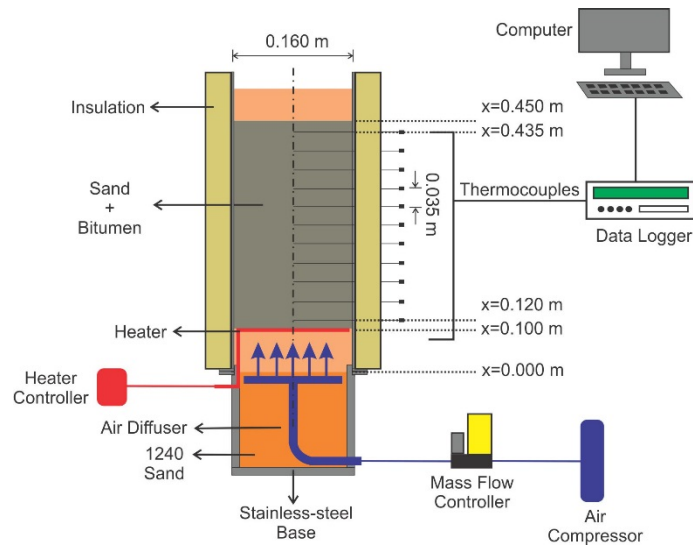


Fig. 1. Schematic of the experimental apparatus.

Table 1.
Smouldering experiments.

Exp. # [-]	u_g [m s ⁻¹]	S_b [%]	t_g^c [s]	t_h^d [s]	Repeats [#]	Self-Sustaining [-]
1	0.025	15	4926	5357	1	Yes
2 ^a	0.058	15	4532±378 ^b	4865±300 ^b	3	Yes
3	0.083	15	5077	5329	1	Yes
4	0.058	10	5486	6004	1	Yes
5	0.058	5	5890	6370	1	Yes
6	0.025	10	4677	5110	1	Yes
7	0.025	5	5100	5700	1	No

^a Base case; ^b 95% confidence interval; ^c time that air flux is turned on (DT=0); ^d time that heater is turned off; ^e peak temperatures are within 2% and front velocities are within 13%, agreeing with extensive studies of smouldering experiment repeats as shown in [34].

2.2. Modelling

A one-dimensional numerical model, validated for robust smouldering [5], was used to simulate smouldering of bitumen mixed with sand following the experimental conditions presented in Table 1. The model was developed in COMSOL Multiphysics with constant mesh size (0.1 mm) and time-step variable,

controlled by COMSOL to meet stability criteria. The computational domain mimics the centre-line of the apparatus with the heater simulated by a constant heat flux ($\dot{q}''=25 \text{ kW m}^{-2}$) delivered at the inlet boundary. The Darcy air flux was initiated at $x=0 \text{ m}$ by a constant u_g . The boundary conditions are identical to those described in detail in [5, 6, 17].

Table 2.
Model Input Parameters

Par.	Value	Unit	Ref.
$\log(A_b)$	7.5	$\log(\text{s}^{-1})$	[5]
$\log(A_c)$	4.9	$\log(\text{s}^{-1})$	[5]
C_{pb}	921	$\text{J kg}^{-1} \text{K}^{-1}$	[35]
D_g	4.53×10^{-5}	$\text{m}^2 \text{s}^{-1}$	[36]
ΔH_b	1.62	MJ kg^{-1}	[5]
ΔH_c	-38.73	MJ kg^{-1}	[5]
E_b	135	kJ mol^{-1}	[5]
E_c	90	kJ mol^{-1}	[5]
k_b	0.15	$\text{W m}^{-1} \text{K}^{-1}$	[37]
k_p	1×10^{-9}	m^2	[32]
ϕ	0.37	-	[32]
R_g	8.314	$\text{J K}^{-1} \text{mol}^{-1}$	[32]
U	13	$\text{W m}^{-2} \text{K}^{-1}$	[5]
v_c	0.55	-	[5]
v_{O_2}	1.70	$\text{kg.O}_2 \text{ kg.fuel}^{-1}$	[5]
σ	5.67×10^{-8}	$\text{W m}^{-2} \text{K}^{-4}$	[32]

The kinetics for bitumen smouldering followed a 2-step mechanism [38]



The reaction rates for pyrolysis (R_b) and oxidation (R_c) were described as first-order Arrhenius reactions:

$$\dot{R}_b = A_b \exp\left(-\frac{E_b}{R_g T_s}\right) (Y_b) \quad (3)$$

$$\dot{R}_c = A_c \exp\left(-\frac{E_c}{R_g T_s}\right) (Y_c)(Y_{O_2})$$

The conservation of mass for solid:

$$\frac{\partial(Y_b)}{\partial t} = -\dot{R}_b \quad (4)$$

$$\frac{\partial(Y_c)}{\partial t} = v_c \dot{R}_b - \dot{R}_c$$

and gas:

$$\frac{\partial(\rho_g \phi_g)}{\partial t} + \frac{\partial(\rho_g u_g)}{\partial x} = (\phi_b \rho_{bT}) \left((1 - v_c) \dot{R}_b + (1 - v_{O_2}) \dot{R}_c \right) \quad (5)$$

phases were included. Eq. (5) solved air pressures and velocities adopting Darcy's Law without gravity effects, and the gas density (ρ_g) followed the ideal gas law. The bulk transport of oxygen was described by:

$$\phi_g \frac{\partial(\rho_g Y_{O_2})}{\partial t} + \frac{\partial(\rho_g u_g Y_{O_2})}{\partial x} = \phi_g \frac{\partial}{\partial x} \left(\rho_g D_g \frac{\partial Y_{O_2}}{\partial x} \right) - (\phi_b \rho_{bT}) v_{O_2} \dot{R}_c \quad (6)$$

The model solved the transient energy equation for both solid (T_s) and gas (T_g) phases:

$$\begin{aligned} (\rho C_p)_{eff} \frac{\partial T_s}{\partial t} = \frac{\partial}{\partial x} \left(k_{eff} \frac{\partial T_s}{\partial x} \right) - U \left(\frac{A_{s,cl}}{V_{cl}} \right) (T_s - T_0) + h_{sg} \left(\frac{A_{s,sp}}{V_{sp}} \right) (T_g - T_s) \\ - (\phi_b \rho_{bT}) (\Delta H_c \dot{R}_c + \Delta H_b \dot{R}_b) \end{aligned} \quad (7)$$

$$\phi_g \left(\rho_g C_{p_g} \right) \frac{\partial T_g}{\partial t} + \rho_g C_{p_g} u_g \frac{\partial T_g}{\partial x} = \phi_g \frac{\partial}{\partial x} \left(k_g \frac{\partial T_g}{\partial x} \right) + h_{sg} \left(\frac{A_{s,sp}}{V_{sp}} \right) (T_s - T_g) \quad (8)$$

where $(\rho C_p)_{eff} = (1 - \phi) \rho_s C_{p_s} + \phi_b \rho_{bT} C_{p_b}$, $k_{eff} = (1 - \phi)(k_s + k_{rad}) + \phi_b k_b$, $\phi = \phi_g + \phi_b$, and $\phi_b = \phi S_b$. Therefore, Local Thermal Non-Equilibrium (LTNE) was considered by applying the interfacial heat transfer coefficient (h_{sg}) according to the empirical Nusselt (Nu) versus Reynolds (Re) and Prandtl

(Pr) correlation developed in [32]. A homogeneous porous medium was assumed and sand particles were taken as spheres “ sp ” ($A_{s,sp}/V_{sp}=6(1-\phi)/d_p$).

Radiation heat transfer (“ rad ”) followed the Rosseland approximation and was expressed as a radiative conductivity ($k_{rad}=16\sigma d_p T_s^3/3$) [32]. A global heat loss coefficient (U) was included and used the surface area per unit volume ($A_{s,cl}/V_{cl}=2/r$) of a cylinder (“ cl ”), where $r = 0.08$ m is the column radius. Thermal properties of air and sand vary with temperature [32], whereas C_{pb} and k_b were assumed constant (Table 2). The average front velocity (v_f) and average peak temperature for each case was calculated according to standard methods [7]. A new fitting of ΔH_c was conducted (note that all the other previously fitted parameters [5] were kept the same, Table 2) based on the methodology developed in [5]. Moreover, a previously developed global energy balance (Eq. (1)) [6, 17] was employed, taking into account the measured ΔH_c from [5] and new fitted ΔH_c for each condition presented in Table 1.

3. Results

3.1. Smouldering Experiments

Figure 2 shows the results for Exp. #1-3 (Table 1). Peak temperature (T_p) had a negligible increase (640-643°C) u_g increased from 0.025 to 0.083 m s⁻¹ and S_b remained constant, whereas front velocity (v_f) increased from 3.27 to 5.05 mm min⁻¹, as predicted in [6]. Figure 2 also shows simulations employing a fixed ΔH_c , measured via DSC experiments [5] (Figs. 2a-d). The predictions match the experiments in terms of T_p and v_f (Fig. 2d) and shape of the temperature curves (less than 25% error), except for the 0.025 m s⁻¹ case. In this weak self-sustaining smouldering case, the model under-predicted v_f by 38% (Fig. 2d) and over-predicted the rate of cooling (26% error) (Fig. 2a). The good prediction of these two more robust cases was also reported previously [5], but this poor prediction of this (and other) less robust cases is new and underlies the central issue explored in this paper.

All of the relevant model variables – U , v_{O_2} , ΔH_c , A , and E – were explored to identify which could lead to an improved prediction of Exp. #1 (results not shown). Only by varying ΔH_c (Fig. 2e) was able to predict both T_p and v_f (Fig. 2h) and the temperature profiles, reducing this error from 26% to 10% (Fig. 2e). Although not necessary for good predictions of the experiments (as shown in [5] and Figs. 2a-d), for completeness ΔH_c was adjusted for the other two robust cases (Figs. 2f-g), which slightly improved their fitting (Fig. 2h).

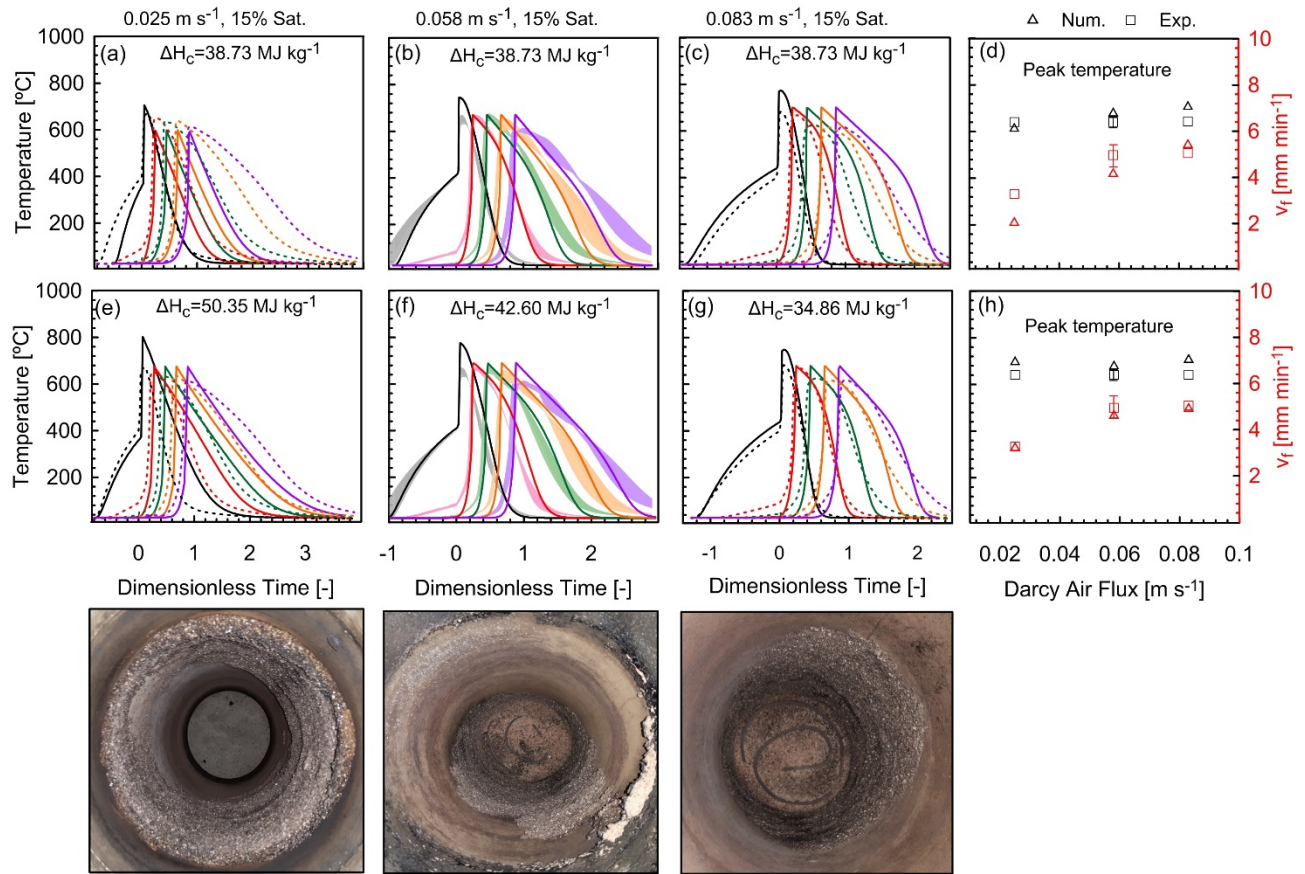


Fig. 2. (Dashed line) Experimental and (solid line) numerical sand/bitumen temperature versus DT for Exp. #1(a,e), 2(b,f), and 3(c,g). Colours in (a-g) show thermocouple positions (x) from 0.12 to 0.40 m with 0.07 m intervals. (b,f) The shadings encompass three experimental repeats. (d, h) T_p and v_f versus u_g . The error bars denote the variation observed in three repeats of Exp. #2, Table 1. Photos show the evolution of the interface between clean sand and crust of pyrolyzed fuel near the column wall, i.e., thick/intact crust (a), thin/crumbling crust (b), effectively no crust (c).

Figure 2 suggests that as the system moves towards less robust conditions (e.g., lower air flux), increasing ΔH_c allows the model to maintain accurate predictions. To explore this unusual and unexpected outcome

further, four additional less robust experiments (Fig. 3) were conducted, considering low (0.025 m s^{-1}) and medium (0.058 m s^{-1}) air flux and low (5%) and medium (10%) fuel saturation (Exps. #4-7, Table 1). T_p for these experiments exhibited low sensitivity (Fig. 4a-b) to a decrease in S_b and u_g for the self-sustaining cases (Exps. #4-6) as shown in Fig. 3. The highest decrease in T_p (from 641 to 571°C) corresponded to reducing S_b from 15% to 5% at 0.058 m s^{-1} (Fig. 4a). v_f showed a different behaviour, i.e., it was insensitive to a decrease in S_b from 15% to 10% at both air fluxes, but when S_b diminished from 10% to 5% at 0.025 m s^{-1} , v_f reduced significantly from 5.40 to 3.72 mm min^{-1} (Fig. 4a). Extinction occurred when S_b was reduced to 5% with 0.025 m s^{-1} air flux (Fig. 3d).

Figures 3a-d compare Exps. #4-7 with simulated temperatures employing the fixed (measured) ΔH_c . All cases exhibited high errors in the temperature predictions, i.e., 33%, 48%, 99%, and 63% respectively. In fact, for Exps. #5 and #6 the model predicts extinction, which is contrary to the experimental results (Figs. 3b,c). Here, ΔH_c was also adjusted but an additional parameter was tested: oxygen mass flux (\dot{m}_{O_2}). Figs. 3f and 3g show that an increase in \dot{m}_{O_2} from 0.28 to 0.50 g s^{-1} and 0.12 to 0.27 g s^{-1} , respectively, enables the reaction to be reactivated, from initially showing extinction behaviour to become self-sustaining. However, this increase in \dot{m}_{O_2} also increases heat losses by convective cooling, i.e., the trailing edge of the temperature curve cools much faster than the experiment; similar behaviour occurs in Fig. 3e. When ΔH_c was varied from 58.10 to 92.95 MJ kg^{-1} , the simulations in Figs. 3i-l matched the experiments well and decreased the errors to 17%, 8%, 18%, and 22%, respectively. Moreover, the model well-predicts T_p and v_f for the self-sustaining cases (Fig. 4). Therefore, although an increase in \dot{m}_{O_2} can reactivate a reaction that is otherwise dying, consequently increasing T_p and v_f , it does not match the experimental data as well as an increase in ΔH_c (Figs. 3i-l), which improves all aspects of the model fitting.

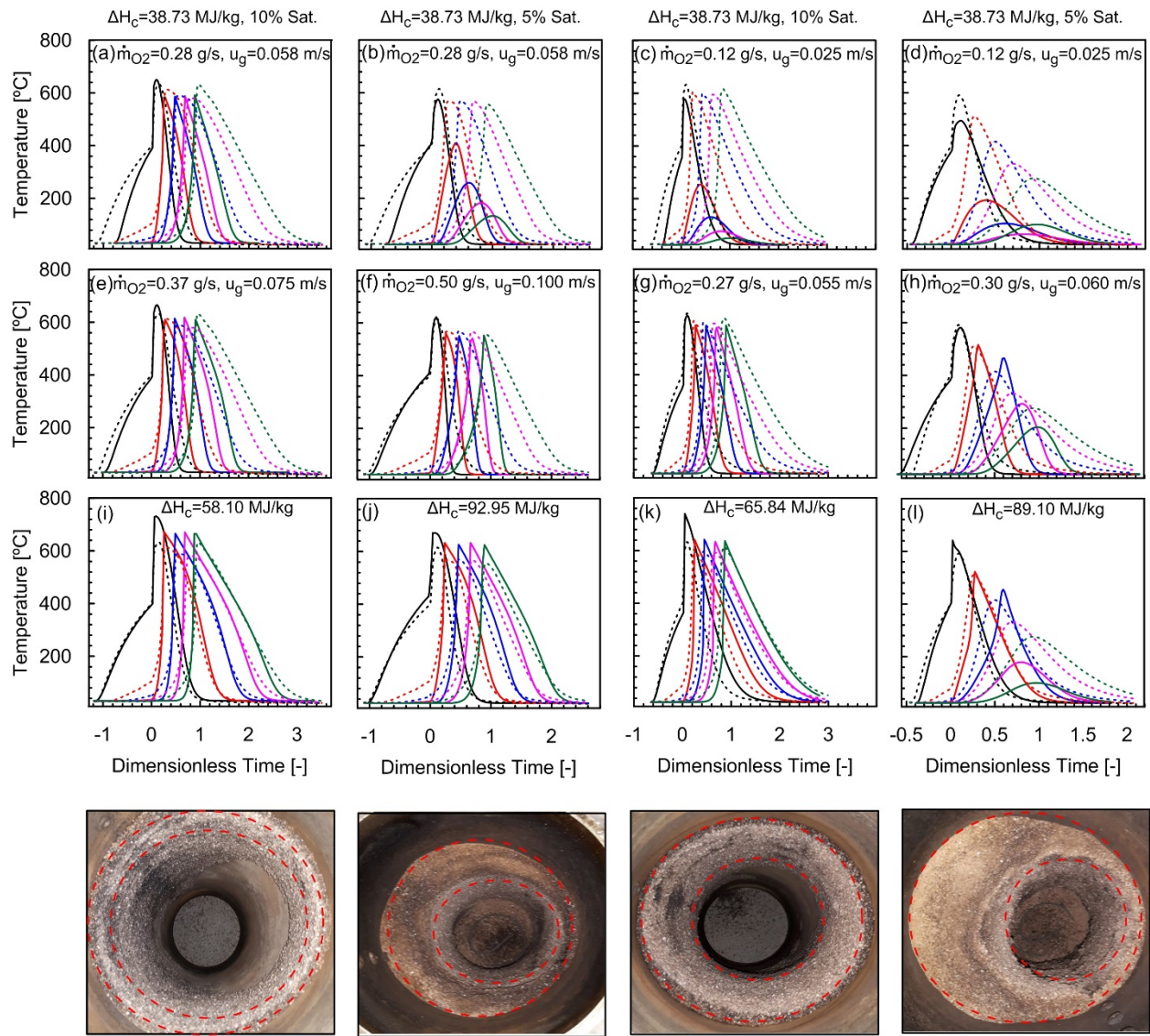


Fig. 3. (Dashed line) Experimental and (solid line) numerical sand/bitumen temperature versus DT for Experiments #4, #5, #6, and #7. Colours show thermocouple positions (x) from 0.12 to 0.40 m with 0.07 m intervals. Photos show the evolution of the interface between clean sand and crust (red dashed circles) of pyrolyzed fuel near the column wall.

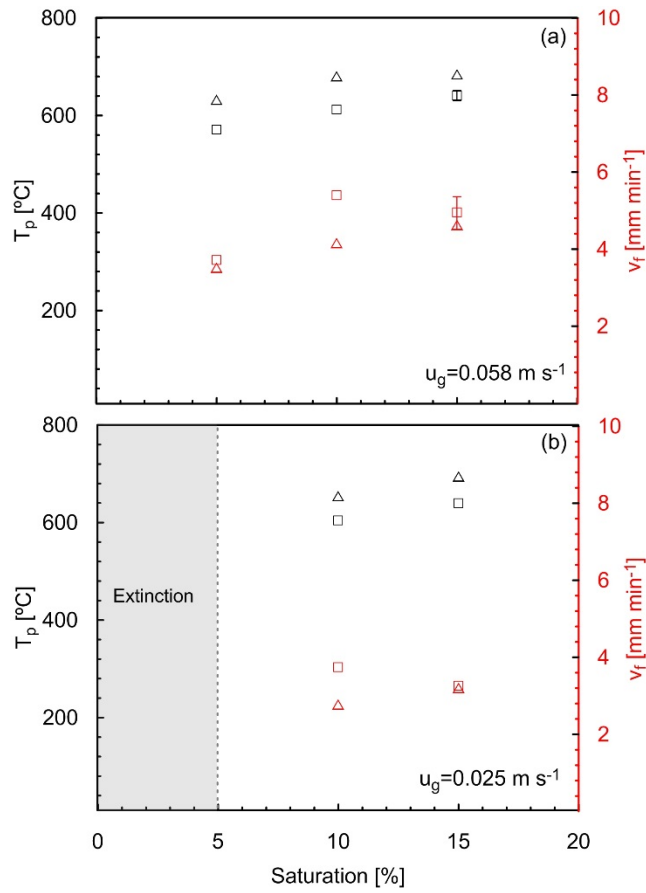


Fig. 4. T_p and v_f versus saturation: (■) experimental and (▲) numerical data. Exp. #2 (Table 1) was added in both figures for comparison and in (b) the error bars denote the variation observed in three repeats. ΔH_c values used are presented in Figs. 2b-d and Figs. 3i-l.

3.2. Net Energy Rate

Figure 5 shows the model-estimated net energy rate (\dot{E}_{net}) at $DT=0.5$ (i.e., when the reaction was half way along the column) for all the experiments listed in Table 1. \dot{E}_{net} was obtained via Eq. (1), employing the measured ΔH_c (open symbols) and the best-fit ΔH_c (closed symbols). The net rate of energy produced needs to exceed zero for a scenario to be self-sustaining and as the rate increases scenarios are more robust [6, 17]. None of the cases are as robust as the top of the range for one-dimensional columns observed in [6] of 5 kJ s⁻¹. It is observed that the two most robust cases (Exps. #2 and #3), which did not require adjusting ΔH_c , exhibit \dot{E}_{net} , 0.9 and 1.4 kJ s⁻¹, respectively. For Exps. #5 and #6 (Figs. 3b and 3c), the

measured ΔH_c resulted in a negative \dot{E}_{net} , predicting extinction, while experiments showed self-sustaining behaviour. This suggests that the net energies predicted for these two cases is too low.

Both modeling and measurements focus on the reactor centre line and assume, given the one-dimensional propagation assumption, that the reaction front is flat and that any deformations are limited to a very small region near the edges. An earlier study [39] showed that deformation in the smouldering front can lead to mixed flow conditions that can redistribute energy in a manner such that it can enhance a smouldering reaction or bring it to extinction. In this case, sufficient net energy was delivered through increasing energy generation at the centre-line by increasing ΔH_c . It is important to note that the increase in the heat of combustion is the only corrective mechanism by which multi-dimensional redistribution of energy can be achieved in a one dimensional model.

Figure 5 shows that when ΔH_c was increased, \dot{E}_{net} increased from 0.20 to 0.88 kJ s⁻¹ for Exp. #3 and increased from negative values (-0.30 and -0.24 kJ s⁻¹) to positive values (0.52 and 0.59 kJ s⁻¹) for Exps. #5 and #6. Moreover, the extinction case (Exp. #7) still exhibits a negative net energy rate (-0.13 kJ s⁻¹), as expected, even when ΔH_c was increased from 38.73 to 89.10 MJ kg⁻¹. In summary, all self-sustaining scenarios show an increase in robustness as air flux and saturation increase. This is consistent with the results reported in [6]. It is acknowledged that due to the lack of perfect fit between the experiment and simulations, \dot{E}_{net} plotted in Fig. 5 is only an approximation of the experimental \dot{E}_{net} .

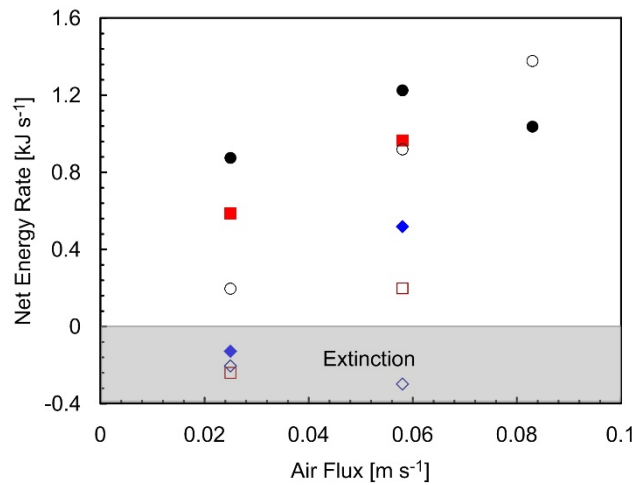


Fig. 5. \dot{E}_{net} at $DT=0.5$ for all scenarios presented in Table 1. Simulations used (open symbols) the measured ΔH_c and (closed symbols) the best-fit ΔH_c as shown in Figs. 2 and 3. Colours show (black) 15% S_b , (red) 10% S_b , and (blue) 5% S_b .

3.3. Discussion on the role of ΔH_c

It is acknowledged that ΔH_c is not expected to vary when the fuel type is fixed. When ΔH_c is measured by DSC, some variability can be expected due to variation in the heating rate. Thus, the ΔH_c derived from those measurements will carry some error. Previous studies have shown that incompleteness of combustion results in ΔH_c being lower than that of complete combustion [22, 36]. However, it is not physically possible for ΔH_c to exceed that of complete combustion as measured by bomb calorimeter (e.g., for bitumen $\Delta H_c=40.95$ MJ kg⁻¹ [40]). Thus, ΔH_c in this context must be understood as a fitting parameter that modifies the energy balance in appropriate ways to reproduce weakly self-sustaining smouldering experiments. The fact that ΔH_c must be increased in less robust systems suggests that the energy balance expressed in Eq. (1) does not actually decrease for these weak scenarios as much as the model predicts.

There is evidence that the assumption of a one-dimensional system may start to fail for weakly self-sustained and extinguishing scenarios. For Exps. #2 and #3, which were relatively robust scenarios, a thin crust of pyrolyzed fuel remained along the column walls after the experiment successfully completed (Figs. 2b and 2c). This can be attributed to lateral heat losses driving extinction near the wall. However, a much thicker crust was observed after smouldering in Exps. #1 (Fig. 2a) and #4-7 (Fig. 3a-d), where ΔH_c had to

be considerably adjusted. This indicates that the smouldering reaction was narrowing within the reactor and that multi-dimensional effects were growing in significance.

The implications are many, all in contrast to the model assumptions: (i) radial heat losses change as the reaction propagates, (ii) the effective radius of the smouldering reaction changes as the reaction propagates, (iii) the centre-line temperatures become more insulated (from larger thickness of inert sand between the reaction and the reactor wall) as the reaction propagates, (iv) the extent and rate of fuel oxidation across the radius changes as the reaction propagates and (v) multi-dimensional flow patterns develop carrying heat from the edges to the centreline as the reaction propagates. All of these would affect the local energy balance at the reaction front as well as the global energy balance of the system.

An important detail is the generation of permeability gradients between the clean zone in the centre of the column (i.e., high permeability) and the pyrolyzed zone near the wall (i.e., low permeability). This creates a front deformation that leads to a redistribution of the air flow, altering the global energy balance at the centre-line. Cold air coming from the bottom of the reactor is convected from the edges of the reactor towards the centreline. Given that the edges are still significantly above ambient temperature, it is very likely that this warm air contributes to the pre-heating of the fuel. It is for this reason that the redistribution of the air flow from the sides towards the centre-line alters the global energy balance in a manner that it mostly affects propagation velocities in the axis of the reactor. The result is faster propagation velocities and a more favorable energy balance at the reaction zone. This, in a one-dimensional system, could be represented by extrinsic energy being added to the reaction zone. This hypothesis was tested by increasing the oxygen mass flux, but resulted in large convective cooling. Therefore, it is hypothesized that, if the model was modified to simulate a fully multi-dimensional system, it may be that these results could be simulated without needing to modify ΔH_c .

It is noted that the model was fit to the experiments allowing both U and ΔH_c to vary. Therefore, it is important to establish if a variation of the heat loss coefficient could serve to correct the observed errors.

Allowing U to vary makes it possible for the model to approximate the change of heat losses between different experiments. However, the influence of U on the peak temperature and smouldering velocity is minor compared to that of ΔH_c (figures not shown). Despite these simulations also fitting the experiments well, they were unable to achieve ΔH_c values less than the bomb calorimeter value. In other words, using U as a fitting parameter does not compensate for or remove the requirement to increase ΔH_c .

The combined results of model and experiments established that the weak smouldering regime is controlled by exactly the same parameters as robust smouldering. The simple two-step kinetic model can reproduce the characteristics of the smouldering front appropriately. Furthermore, a simple fit of the heat of combustion is capable of correcting the discrepancies induced by the three-dimensional front and the consequent three-dimensional flow field. The heat of combustion, as defined here, must therefore be understood as an effective value that mixes heat generated by combustion and heat transfer. This correction manages to amalgamate changes in heat and mass transfer as well as permeability and heat losses into a single parameter showing that the overall impact of all these changes is dominated by the net transfer of heat from the edges to the centreline.

From a practical perspective, these results are extremely important, because they demonstrate that detailed three-dimensional modelling might not be necessary to predict the main (i.e., centreline) characteristics of the weak smouldering regime. Three-dimensional modelling represents an enormous challenge because it requires not only the full resolution of the transport equations in three-dimensions, but the resolution of the coupled effects of the changes in permeability of the porous media, fuel consumption and fuel transformation into the observed crust. The formation of a crust adds a final process that needs to be considered, which involves extinction chemistry. All of these effects need to be modelled simultaneously because they define the solution of the transport equations, and the solution of the transport equations defines these processes. Currently, none of the published models can predict these coupled effects.

4. Conclusions

In engineered smouldering applications, it is preferred to create self-sustaining scenarios that are robust, i.e., far from extinction. In this work, smouldering column experiments were conducted and spanned conditions from robust self-sustaining through weak self-sustaining and to extinction by systematically lowering the applied air flux and the fuel concentration. These were demonstrated to represent a range of global net energy rates from negative (extinction) to approximately 1.4 kJ s^{-1} . Experimental results were predicted with a one-dimensional numerical model previously validated against a robust experiment. Under robust conditions, the use of a measured heat of combustion provided predictions that were in good agreement with experiments in terms of temperature predictions and front velocity. Under weak and extinction conditions, the model was unable to accurately reproduce experiments unless the heat of combustion was increased from 34.86 to 92.95 MJ kg^{-1} . This value exceeds the bomb calorimeter measurement, which is not physically possible. Therefore, the heat of combustion in such models can be understood as an effective value that amalgamates the heat released by smouldering but also a complex set of heat and mass transfer processes. Currently, there is no model that is capable of predicting smouldering processes near extinction; therefore, the fact that a single fitting parameter can allow the use of the same formulation to predict smouldering in both the robust and weak regimes is of extreme practical importance. Thus, this work reveals the value of considering the heat of combustion as a single fitting parameter.

Acknowledgements

Funding was provided by the Natural Sciences and Engineering Research Council of Canada (Grant Nos. CREATE 449311-14, RGPIN 2018-06464 and RGPAS-2018-522602).

References

- [1] T.J. Ohlemiller, Modeling of smoldering combustion propagation, *Prog. Energy Combust. Sci.* 11 (1985) 277-310.
- [2] R.M. Hadden, G. Rein, C.M. Belcher, Study of the competing chemical reactions in the initiation and spread of smouldering combustion in peat, *Proc. Combust. Inst.* 34 (2013) 2547-2553.

- [3] P. Pironi, C. Switzer, G. Rein, A. Fuentes, J.I. Gerhard, J.L. Torero, Small-scale forward smouldering experiments for remediation of coal tar in inert media, *Proc. Combust. Inst.* 32 (2009) 1957-1964.
- [4] P. Pironi, C. Switzer, J.I. Gerhard, G. Rein, J.L. Torero, Self-Sustaining Smoldering Combustion for NAPL Remediation: Laboratory Evaluation of Process Sensitivity to Key Parameters, *Environ. Sci. Technol.* 45 (2011) 2980-2986.
- [5] M.A.B. Zanoni, J.L. Torero, J.I. Gerhard, The role of local thermal non-equilibrium in modelling smouldering combustion of organic liquids, *Proc. Combust. Inst.* 37 (2019) 3109-3117.
- [6] M.A.B. Zanoni, J.L. Torero, J.I. Gerhard, Delineating and explaining the limits of self-sustained smouldering combustion, *Combust. Flame* 201 (2019) 78-92.
- [7] C. Switzer, P. Pironi, J.I. Gerhard, G. Rein, J.L. Torero, Self-sustaining smoldering combustion: A novel remediation process for non-aqueous-phase liquids in porous media, *Environ. Sci. Technol.* 43 (2009) 5871-5877.
- [8] T.L. Rashwan, J.I. Gerhard, G.P. Grant, Application of self-sustaining smouldering combustion for the destruction of wastewater biosolids, *Waste Manage.* 50 (2016) 201-212.
- [9] L. Yermán, H. Wall, J. Torero, J.I. Gerhard, Y.L. Cheng, Smoldering Combustion as a Treatment Technology for Feces: Sensitivity to Key Parameters, *Combust. Sci. Technol.* 188 (2016) 968-981.
- [10] H.K. Wyn, M. Konarova, J. Beltramini, G. Perkins, L. Yermán, Self-sustaining smouldering combustion of waste: A review on applications, key parameters and potential resource recovery, *Fuel Process. Technol.* 205 (2020) 106425.
- [11] A. Serrano, H. Wyn, L. Dupont, D.K. Villa-Gomez, L. Yermán, Self-sustaining treatment as a novel alternative for the stabilization of anaerobic digestate, *J. Environ. Manage.* 264 (2020) 110544.
- [12] G. Gianfelice, M. Della Zassa, A. Biasin, P. Canu, Onset and propagation of smouldering in pine bark controlled by addition of inert solids, *Renewable Energy* 132 (2019) 596-614.
- [13] S. Saberi, K. Samiei, E. Iwanek, S. Vohra, M. Farkhondehkavaki, Y.-L. Cheng, Treatment of fecal matter by smoldering and catalytic oxidation, *Journal of Water, Sanitation and Hygiene for Development*, doi:10.2166/washdev.2020.120(2020).
- [14] I. Fabris, D. Cormier, J.I. Gerhard, T. Bartczak, M. Kortschot, J.L. Torero, Y.-L. Cheng, Continuous, self-sustaining smouldering destruction of simulated faeces, *Fuel* 190 (2017) 58-66.
- [15] M.F. Martins, S. Salvador, J.F. Thovert, G. Debenest, Co-current combustion of oil shale - Part 2: Structure of the combustion front, *Fuel* 89 (2010) 133-143.
- [16] L. Yermán, H. Wall, J.L. Torero, Experimental investigation on the destruction rates of organic waste with high moisture content by means of self-sustained smoldering combustion, *Proc. Combust. Inst.* 36 (2017) 4419-4426.
- [17] M.A.B. Zanoni, J.L. Torero, J.I. Gerhard, Determining the conditions that lead to self-sustained smouldering combustion by means of numerical modelling, *Proc. Combust. Inst.* 37 (2019) 4043-4051.
- [18] A.P. Aldushin, I.E. Rumanov, B.J. Matkowsky, Maximal energy accumulation in a superadiabatic filtration combustion wave, *Combust. Flame* 118 (1999) 76-90.
- [19] D.A. Schult, B.J. Matkowsky, V.A. Volpert, A.C. Fernandez-Pello, Propagation and extinction of forced opposed flow smolder waves, *Combust. Flame* 101 (1995) 471-490.
- [20] D.A. Schult, B.J. Matkowsky, V.A. Volpert, A.C. Fernandez-Pello, Forced forward smolder combustion, *Combust. Flame* 104 (1996) 1-26.
- [21] J.L. Torero, A.C. Fernandez-Pello, D. Urban, Experimental observations of the effect of gravity changes on smoldering combustion, *AIAA Journal* 32 (1994) 991-996.
- [22] S.V. Leach, G. Rein, J.L. Ellzey, O.A. Ezekoye, J.L. Torero, Kinetic and fuel property effects on forward smoldering, *Combust. Flame* 120 (2000) 346-358.
- [23] M. Sennoune, S. Salvador, M. Quintard, Toward the Control of the Smoldering Front in the Reaction-Trailing Mode in Oil Shale Semicoke Porous Media, *Energy Fuels* 26 (2012) 3357-3367.

- [24] G. Baud, S. Salvador, G. Debenest, J.-F. Thovert, New Granular Model Medium To Investigate Smoldering Fronts Propagation—Experiments, *Energy Fuels* 29 (2015) 6780-6792.
- [25] B.-s. Jia, M.-z. Xie, H. Liu, Numerical study on the propagation characteristics of forward smoldering in a cellulosic packed bed, *J. Shanghai Univ.(Engl. Ed.)* 12 (2008) 171-179.
- [26] J. Yang, H. Chen, N. Liu, Heat Loss and Kinetic Effects on Extinction and Critical Self-Sustained Propagation of Forced Forward Smoldering, in: K. Harada, K. Matsuyama, K. Himoto, Y. Nakamura, K. Wakatsuki (Eds.), *Fire Science and Technology 2015: The Proceedings of 10th Asia-Oceania Symposium on Fire Science and Technology*, Springer Singapore, Singapore, 2017, pp. 831-840.
- [27] H. Fadaei, M. Sennoune, S. Salvador, A. Lapene, G. Debenest, Modelling of non-consolidated oil shale semi-coke forward combustion: Influence of carbon and calcium carbonate contents, *Fuel* 95 (2012) 197-205.
- [28] V. Pozzobon, G. Baud, S. Salvador, G. Debenest, Darcy Scale Modeling of Smoldering: Impact of Heat Loss, *Combust. Sci. Technol.* 189 (2017) 340-365.
- [29] X. Huang, G. Rein, Upward-and-downward spread of smoldering peat fire, *Proc. Combust. Inst.* 37 (2019) 4025-4033.
- [30] G. Debenest, V.V. Mourzenko, J.F. Thovert, Smoldering in fixed beds of oil shale grains. A three-dimensional microscale numerical model, *Combust. Theor. Model.* 9 (2005) 113-135.
- [31] G. Pablo, M. Christian, W. Cindy, Numerical Model to Quantify the Influence of the Cellulosic Substrate on the Ignition Propensity Tests, *Beiträge zur Tabakforschung International/Contributions to Tobacco Research* 27 (2016) 102-112.
- [32] M.A.B. Zanoni, J.L. Torero, J.I. Gerhard, Determination of the interfacial heat transfer coefficient between forced air and sand at Reynold's numbers relevant to smoldering combustion, *Int. J. Heat Mass Transfer* 114 (2017) 90-104.
- [33] L. Kinsman, J.L. Torero, J.I. Gerhard, Organic liquid mobility induced by smoldering remediation, *J. Hazard. Mater.* 325 (2017) 101-112.
- [34] A.L. Duchesne, Smoldering Combustion Treatment of Soils and Granular Activated Carbon Contaminated with Per- and Polyfluoroalkyl Substances, Western University, Electronic Thesis and Dissertation Repository. 6878., 2020.
- [35] R.H. Perry, D.W. Green, *Perry's Chemical Engineers' Handbook*, 7th ed., McGraw-Hill, New York, USA, 1999.
- [36] J.L. Torero, A.C. Fernandez-Pello, M. Kitano, Opposed Forced Flow Smoldering of Polyurethane Foam, *Combust. Sci. Technol.* 91 (1993) 95-117.
- [37] S.K. Elam, I. Tokura, K. Saito, R.A. Altenkirch, Thermal conductivity of crude oils, *Exp. Therm Fluid Sci.* 2 (1989) 1-6.
- [38] M.A.B. Zanoni, G. Rein, L. Yermán, J.I. Gerhard, Thermal and oxidative decomposition of bitumen at the Microscale: Kinetic inverse modelling, *Fuel* 264 (2020) 116704.
- [39] J.L. Torero, A.C. Fernandez-Pello, Forward smolder of polyurethane foam in a forced air flow, *Combust. Flame* 106 (1996) 89-109.
- [40] V.M. Abbasov, F.F. Mamedov, T.A. Ismailov, Heats of combustion of oil shale, bitumen, and their mixtures, *Soil Fuel Chem.* 42 (2008) 248-250.